

Introduction to onsemi High Current Dual Half Bridge Modules for Automotive Mild Hybrid Applications

AND90235/D

Series of Modules Available

onsemi has introduced a series of isolated 80 V MOSFET modules in a variety of packages that are suitable for 48 V battery-driven mild hybrid electric vehicles (MHEV) and low voltage traction systems. The series offers options for the insulating ceramic DBC substrate to provide standard and premium thermal performance, various $R_{DS(on)}$ ratings to match the end user's current requirements, and a variety of pin-out options to enable different system designs. The entire series of modules is qualified to AQG324 Recommended Practice, manufactured with AEC-Q101-qualified components. This series of modules further augments onsemi's line of high performance, high reliability transfer-molded modules for automotive applications.

Available Part Numbers and Brief Description

All modules are configured as dual half bridges, a.k.a. 2-phase modules, which are easily connected externally to form a single half bridge suitable for twice the phase current, according to the schematic of Figure 2. Therefore, according to the end user's requirements, three modules may be configured to drive a 3-phase motor or 6-phase motor. The series consists of the following part numbers:

- NXV08H250DT1 – Al_2O_3 substrate with maximum 0.762 m Ω $R_{DS(ON)}$ at 25°C with Standard Pins
- NXV08H250DPT2 – Al_2O_3 substrate with maximum 0.710 m Ω $R_{DS(ON)}$ at 25°C with Pressfit Pins
- NXV08H300DT1 – Al_2O_3 substrate with maximum 0.580 m Ω $R_{DS(ON)}$ at 25°C with Standard Pins
- NXV08H350XT1 – HAIN substrate with maximum 0.762 m Ω $R_{DS(ON)}$ at 25°C with Standard Pins
- NXV08H400XT1 – HAIN substrate with maximum 0.580 m Ω $R_{DS(ON)}$ at 25°C with Standard Pins
- NXV08H400XT2 – HAIN substrate with maximum 0.580 m Ω $R_{DS(ON)}$ at 25°C with Side PCB-Mount Pins

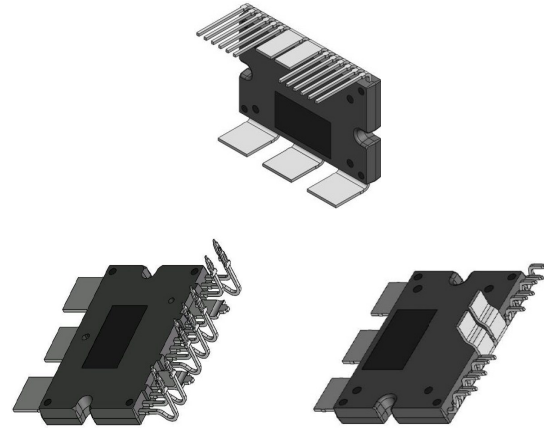


Figure 1. Package Varieties: Standard, Pressfit, and Side PCB-Mount Pins

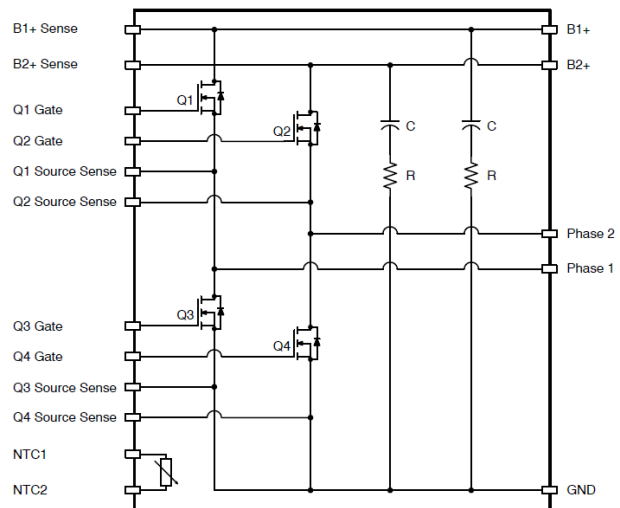


Figure 2. Module Schematic

INTRODUCTION

The NXV08HxxxTz series¹ of automotive power modules (APM) has been designed specifically for high current, high power density designs of 48 V mild hybrid electric vehicle and low voltage traction applications. Belt starter generator systems (in which the electric machine is mounted on the vehicle’s front end accessory drive belt) and integrated starter generator systems (in which the electric machine is integrated into the gearbox) are equally well-served by this series of modules. Three modules may be configured to drive 3-phase or 6-phase motors as illustrated in Figure 3.

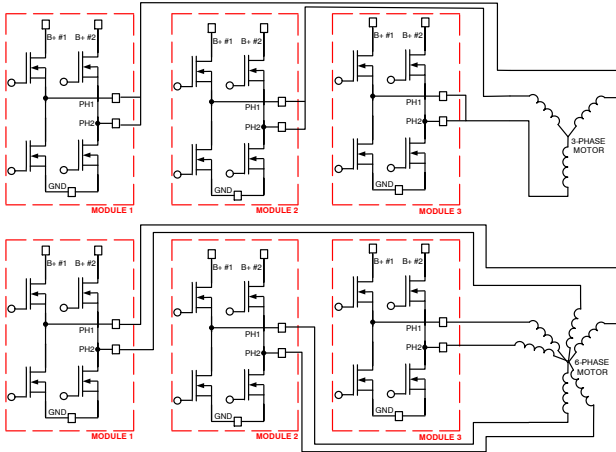


Figure 3. 3- and 6-phase Motor Drive Arrangements

The transfer molded body with integrated, electrically isolated DBC ceramic substrate provides robust reliability and high thermal performance, suitable for bolted or clamped assembly to a heatsink. Power leads are suitable for welding to the assembly’s bus bar structure for low inductance connection to the dc link input filter. Signal leads are available in solderable and pressfit configurations.

These modules are rated for ambient temperature range -40°C to 125°C, and the maximum junction temperature is 175°C. High voltage isolation is tested to 3 kVac for 1 second. Each module is fitted with a temperature-sensing NTC with 25°C value of 10 kΩ, and dual RC snubbers (1 Ω, 15 nF) closely coupled to the MOSFET half bridges for good switching noise suppression.

To enable a variety of motor drives to use the best-suited module, **onsemi** has designed this range of modules with various thermal impedances and MOSFET on-resistance values. With die size variations and substrate material selections, we have provided modules with maximum 25°C R_{DS(ON)} values between 0.58 and 0.762 mΩ and junction-to-case thermal resistance values between 0.19 and 0.54°C/W. Later in the application note we will demonstrate potential system level performance achievable with these modules.

¹ “xxx” refers to approximate current rating, “y” refers to the DBC substrate (D = Al₂O₃, X = HALN), and “z” refers to the pin configuration.

Further technical details for each module are provided in the module data sheets available at www.onsemi.com.

APPLICATION ANALYSIS FOR USE OF APM17 MODULES

Automotive engineers involved in the design of electrified powertrains, including MHEV and light vehicle electric propulsion systems, recognize that there are many trade-offs to be performed and many competing requirements to be met to achieve a high performance, low cost, highly reliable electric drive system. Here we are assuming a 48 V power net is provided, which may be effectively inverted with 80 V rated MOSFETs. This assumption implies proper management of the charging and discharging of the battery to maintain the dc input voltage within the constraints of vehicle manufacturer standards, e.g., ISO21780 [1], keeping low total power loop inductance, and properly monitoring the bus voltage.

Starter/generator applications typically result in several operating modes that have different current requirements. These include continuous and peak power, engine cranking, hill hold, and active short circuit. End users specify the engine cranking torque required to start the engine and an active short circuit mode to protect the inverter and maintain control of the dc link voltage in the event of a fault. There may be other operating points that are not included here.

Continuous and Peak Power

Continuous power requirements range from 5 kW to 15 kW for these systems, with transient peak power conditions as high as 25 kW. With the nominal range of DC voltages for unlimited operation of the motor drive from 36 V to 52 V [1], for the mentioned power levels we can say that maximum continuous phase currents will fall in the range shown in Table 1.

Table 1. Phase Current Required for Range of Power

Battery Voltage	Constant Power Assumptions				Space Vector PWM			
	Cont Shaft Power, kW	Inverter Efficiency %	Motor Efficiency %	Power Factor	Peak AC Power, kW	Line-to-Line RMS Voltage, V	Phase Current, A(RMS)	Phase Current, A(Peak)
36	5.0	95%	95%	90%	5.26	25	133	188
	15.0				15.79	25	398	563
	25.0				26.32	25	663	938
48	5.0	95%	95%	90%	5.26	34	99	141
	15.0				15.79	34	298	422
	25.0				26.32	34	497	703
52	5.0	95%	95%	90%	5.26	37	92	130
	15.0				15.79	37	275	390
	25.0				26.32	37	459	649

Engine Cranking

Engine cranking refers to the operation of starting the combustion engine. Since the engine is not yet rotating, motor RPM will start at zero (stall), and increase in response to the starting torque until it reaches a speed sufficient for the combustion engine to run. Depending on the gear ratio between BSG/ISG machine and the combustion engine, motor RPM will reach perhaps as high as 3000 rpm at the end of the cranking operation. Typically, the current amplitude will be about the same as peak power level for ~300 msec

and then reduced to near continuous power levels for another 500 msec to 2 sec. An example of an engine cranking current profile is given in Figure 4.

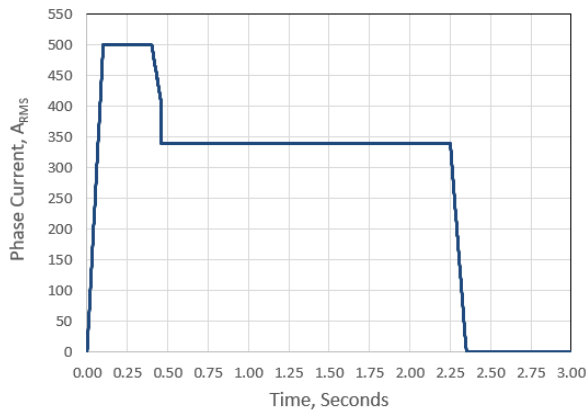


Figure 4. Example Starting Current Profile

Hill Hold

Hill hold refers to the situation where the BSG/ISG is used to mimic the conventional vehicle behavior when stopped on an incline, where the engine’s idling speed and torque operate through the torque converter to produce enough torque to hold the vehicle still on the incline, without the use of the friction brakes.

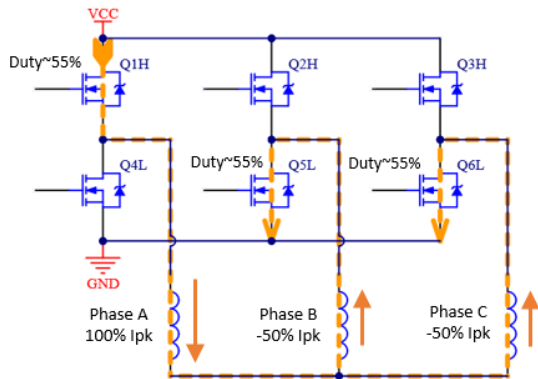


Figure 5. Example Hill Hold Current PWM Pattern

Under these conditions, for a three phase BSG/ISG motor, stall current is required for the duration of the event, and the duty cycle of the PWM will have a particular pattern slightly above 50% duty. The worst-case condition will occur when the rotor is at an angular position such that one phase is at the peak of the sinewave current and the other two phases are at -1/2 peak. This can be represented simply as shown in Figure 5, where we assume Phase A is at peak current.

Active Short Circuit

Active short circuit (ASC) refers to the intentional shorting together of the motor terminals via the inverter switches (either all upper switches or all lower switches) to suppress the back-EMF of the motor under some detected

fault conditions. Suppressing the back-EMF at high motor speeds is particularly important to avoid an over-voltage condition on the inverter components that would otherwise destroy them. Welchko, et al [2], provides details of this operation from the point of view of motor design for interior permanent magnet synchronous machines, but the end user will have to determine the detailed conditions appropriate for their specific motor design and operating conditions. For the purposes of our examples, we will refer to Figure 6, which is taken from [2], and assume a steady state ASC current of 150% of the rated phase current given in Table 1, with a transient peak of 200% of rated, lasting 10 msec.

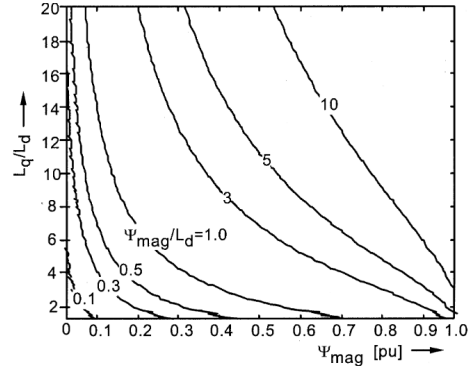


Fig. 19. Contour plot of maximum steady-state three-phase short circuit current ($= \Psi_{mag}/L_d$) in per unit as a function of IPM machine design parameters.

Figure 6. Steady State 3-Phase ASC Current (from [2])

COOLING SYSTEM AND THERMAL RESPONSE

Depending on the application, the higher power systems will likely be liquid cooled, and we may expect nominal coolant temperatures to be in the range of 65°C to 105°C.

End users will approach the heat sinking of the modules in a way consistent with their system design concept. A common approach is to employ an aluminum casting with flat surface for module mounting with the reverse side containing pin-fins submerged into the coolant fluid flow, e.g., as shown in Figure 7.

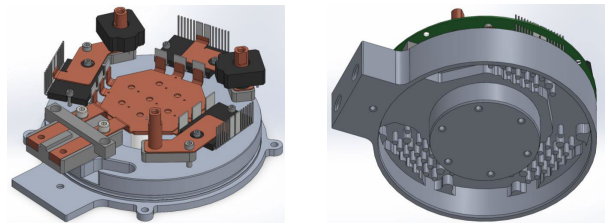


Figure 7. Example Heatsink and Busbar Assembly

Of key importance in assessing the module performance in the application is to obtain the transient thermal response from the module MOSFET junction-to-coolant to ensure that the MOSFETs remain below the data sheet value for $T_{J(MAX)} = 175^\circ\text{C}$. End user designs will vary depending on

numerous factors such as thickness of the aluminum, specific aluminum alloy, pin-fin shape and density, coolant channel shape, coolant flow rate, coolant chemistry, thermal interface material used to mount the module, mounting pressure or screw torque, etc. Each end user will optimize their own system to achieve their design goals. For purposes of analysis in this application note, we will consider a typical design.

onsemi has used CFD analysis and testing to determine the junction-to-case transient thermal impedance for each module, and publishes the maximum value, R_{thjc} , in the data sheets. Table 2 summarizes this value for each part number. The transient thermal impedance, Z_{thjc} , is conveniently represented by a Cauer or Foster thermal RC network which is easily used in circuit simulation or dynamic analysis to assess the junction temperature. An example Z_{thjc} curve is given in Figure 8, while Table 3 provides the Cauer network RC values to represent each module part number thermal response.

Table 2. DATA SHEET VALUES FOR MAX R_{thjc} PER SINGLE FET

Part Number	Max	Units
NXV08H250DT1	0.54	°C/W
NXV08H250DPT2	0.53	°C/W
NXV08H300DT1	0.49	°C/W
NXV08H350XT1	0.21	°C/W
NXV08H400XT1	0.19	°C/W
NXV08H400XT2	0.19	°C/W

As an example, we examine the transient thermal response of the NXV08H400XT1 module. From CFD software and confirmed by testing, we obtained the Z_{thjc} curve shown in Figure 8. From this time response curve, a Cauer RC network can be found to represent the physical behavior of the module. We select the Cauer network so that it can be “cascaded” with the end user’s network representing their heatsink design.

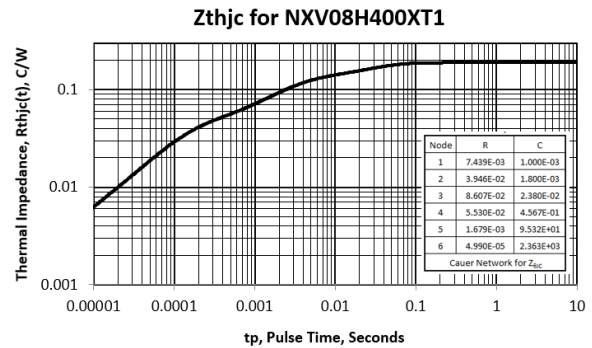


Figure 8. Z_{thjc} Reference Curve, NXV08H400XT1/XT2

The values for the thermal-equivalent RC Cauer network to represent the six modules are given in Table 3. For completeness and reference, Table 4 provides the Foster network RC values.

For interested readers there is a thorough reference application note AND90096/D [3] available at www.onsemi.com on the proper techniques for using onsemi electrothermal MOSFET simulation models (so-called 5-pin or 6-pin models) in concert with external system-level thermal networks as, for example, for a liquid cooled heatsink.

Table 3. MODULE $Z_{thjc}(t)$ CAUER RC NETWORK VALUES

Node	NXV08H250DT1		NXV08H250DPT2		NXV08H300DT1		NXV08H350XT1		NXV08H400XT1/XT2	
	R, Ω	C, F	R, Ω	C, F	R, Ω	C, F	R, Ω	C, F	R, Ω	C, F
1	2.114E-02	3.520E-04	2.075E-02	3.586E-04	6.098E-03	1.190E-03	8.221E-03	9.094E-03	7.439E-03	1.000E-03
2	1.121E-01	6.250E-04	1.101E-01	6.369E-04	3.041E-02	2.261E-03	4.361E-02	1.607E-03	3.946E-02	1.800E-03
3	2.446E-01	8.363E-03	2.401E-01	8.521E-03	7.733E-02	4.884E-02	9.513E-02	2.150E-02	8.607E-02	2.380E-02
4	1.572E-01	1.607E-01	1.542E-01	1.637E-01	3.635E-01	6.507E-02	6.113E-02	4.132E-01	5.530E-02	4.567E-01
5	4.770E-03	3.355E+01	4.683E-03	3.417E+01	9.488E-03	2.254E+01	1.855E-03	8.625E+01	1.679E-03	9.532E+01
6	1.419E-04	8.298E+02	1.392E-04	8.463E+02	3.178E-3	4.624E+01	5.500E-05	2.141E+03	4.990E-05	2.363E+03

Table 4. MODULE $Z_{thjc}(t)$ FOSTER RC NETWORK VALUES

Node	NXV08H250DT1		NXV08H250DPT2		NXV08H300DT1		NXV08H350XT1		NXV08H400XT1/XT2	
	R, Ω	C, F	R, Ω	C, F	R, Ω	C, F	R, Ω	C, F	R, Ω	C, F
1	8.008E-03	5.795E-04	7.860E-03	5.905E-04	2.428E-03	1.910E-03	3.114E-03	1.490E-03	2.818E-03	1.647E-03
2	9.987E-02	1.002E-03	9.802E-02	1.021E-03	2.976E-02	3.369E-03	3.884E-02	2.576E-03	3.514E-02	2.848E-03
3	2.388E-01	9.043E-03	2.344E-01	9.214E-03	2.304E-02	9.333E-02	9.288E-02	2.325E-02	8.403E-02	2.570E-02
4	1.861E-01	1.435E-01	1.826E-01	1.462E-01	4.156E-01	1.065E-01	7.236E-02	3.690E-01	6.547E-02	4.078E-01
5	6.360E-03	2.760E+01	6.242E-03	2.812E+01	1.577E-02	2.166E+01	2.473E-03	7.096E+01	2.238E-03	7.843E+01
6	8.526E-04	1.567E+02	8.369E-04	1.291E+02	3.442E-03	2.691E+01	3.316E-04	3.259E+02	3.000E-04	3.602E+2

ASSESSING MODULE PERFORMANCE UNDER APPLICATION CONDITIONS

Assessing the performance of these modules in a motor drive or other application may be done in various ways. Here we describe a bottom-up simulation effort that makes use of **onsemi** physical and scalable models [4] available at www.onsemi.com for pSpice [5], SIMetrix [6], and LTSpice [7] (and other simulators upon request). These are highly accurate dynamic models that may be employed to evaluate the product prior to the availability of any hardware.

By “bottom-up” we mean that the reader may use circuit simulation or data sheet information to create a suitable module model and exercise that model with usage profiles in a manner to obtain insights into how well the module will meet their requirements. In this section we describe in detail this process.

Module Basic Electrical and Thermal Performance

To evaluate the electrical performance of the module, a circuit simulator like SIMetrix [6] can be used. **onsemi** uses ANSYS Q3D [8] to determine a parasitic model of the package, which is verified by test. Figure 9 shows a simplified version of the module model for the NXV08H400XT1 as an example.

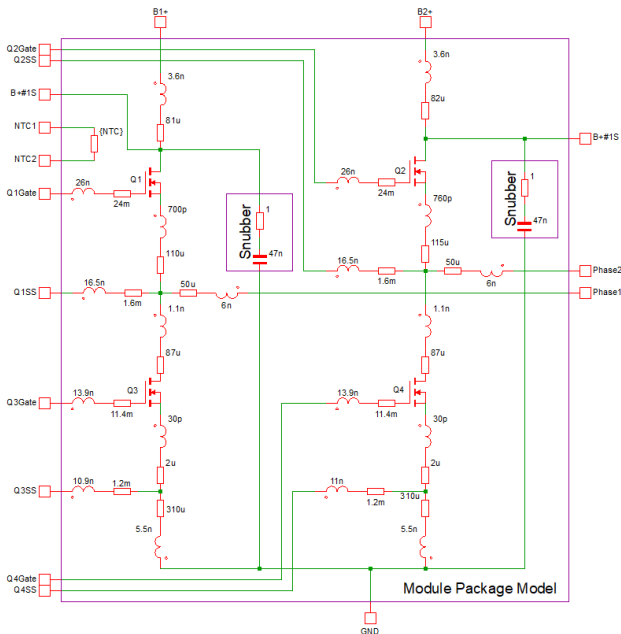


Figure 9. Simplified NXV08H400XT1 Package Model in SIMetrix

Such a model provides a means to evaluate conduction and switching losses and obtain information about drain and gate waveforms. To use this model correctly, a bare die model of the 80 V MOSFETs must be obtained from **onsemi**. External to the schematic shown in Figure 9 the user must add a gate drive circuit and power supply for 48 V, with parasitic stray inductance as appropriate to represent

the user’s bus bar and filtering design. For the purposes of discussion here, the bus bar and 48 V power distribution is modeled as shown in Figure 10. A suitable value for Cbulk is 3 mF to 5 mF, and for LS a good layout will yield stray inductance on the order of 5 nH.

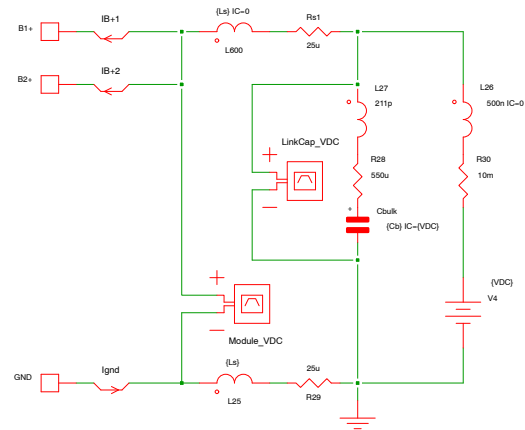


Figure 10. 48 V Battery and Bus Bar Simulation Model

By way of example, the gate drive circuit model shown in Figure 11 can be used. The reader can use this circuit to initiate a simulation, modifying it to represent their design as it evolves, in order to meet their own performance targets.

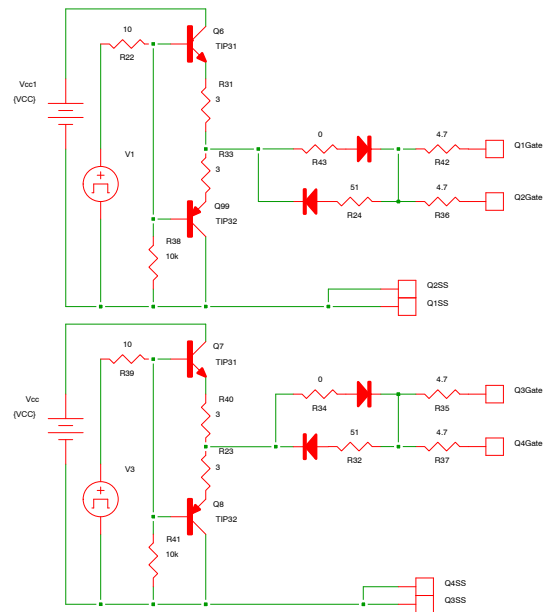


Figure 11. Representative Gate Drive Circuitry

Such a set of schematics can be used to produce a variety of results, including classic two-pulse switching waveforms that are useful for extracting switching energy curves, or for evaluating the variation of $R_{DS(on)}$ as a function of T_j . This information could then be used in a system simulation as

might be implemented in Matlab [9] or a spreadsheet, for example.

With the simulation process described above, a user can develop the necessary information needed to perform system level simulations of a motor drive to determine which module best meets their requirements. **onsemi** has carried out both simulation and tests to acquire comparable data for use in an Excel®-based system analysis tool. The parameters needed for this system analysis include $R_{DS(on)}$ as a function of junction temperature, total switching energy for the desired gate drive, dc link voltage, and parasitic impedance conditions, and the thermal impedance function from junction to desired reference temperature (case, heat sink, or coolant).

For the purposes of this application note, we have collected data for junction-coolant thermal impedance for an assembly similar to that shown in Figure 7. Salient features of the example heat sink assembly are: 3 mm thick aluminum plate with a thermal interface material applied 30 μ m thick with thermal conductivity of 2.1 W/(m-K). With these assumptions, the steady state values of thermal resistance from junction to coolant are shown in Table 5.

An example of the transient thermal impedance curve for the NXV08H400XT1 mounted on the described heat sink is shown in Figure 12. Similar data has been collected for all the model part numbers and the thermal equivalent Cauer and Foster network values are given in Tables 6 and 7.

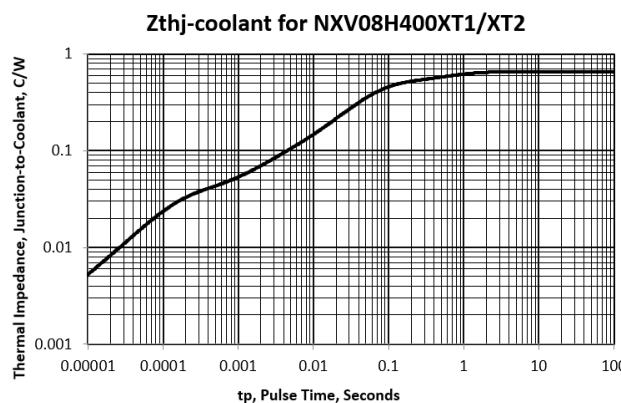


Figure 12. Transient Thermal Impedance Junction-Coolant for NXV08H400XT1/XT2 Module

Table 5. THERMAL RESISTANCE, JUNCTION TO COOLANT

Part Number	Max	Units
NXV08H250DPT2/DT1	0.969	°C/W
NXV08H300DT1	0.860	°C/W
NXV08H350XT1	0.755	°C/W
NXV08H400XT1/XT2	0.656	°C/W

Table 6. MODULE Zthj-coolant(t) CAUER RC NETWORK VALUES

Node	NXV08H250DT1/DPT2		NXV08H300DT1		NXV08H350XT1		NXV08H400XT1/XT2	
	R, Ω	C, F	R, Ω	C, F	R, Ω	C, F	R, Ω	C, F
1	6.720E-03	1.086E-03	5.321E-03	1.372E-03	7.141E-03	1.019E-03	6.205E-03	1.173E-03
2	3.513E-02	2.014E-03	2.763E-02	2.585E-03	3.606E-02	1.924E-03	3.134E-02	2.214E-03
3	1.140E-01	2.785E-02	9.660E-02	3.416E-02	9.162E-02	3.508E-02	7.959E-02	4.038E-02
4	5.663E-01	5.175E-02	4.924E-01	5.774E-02	4.502E-01	6.635E-02	3.912E-01	7.637E-02
5	2.414E-01	2.443E+00	2.326E-01	2.497E+00	1.663E-01	3.510E+00	1.445E-01	4.040E+00
6	5.312E-03	2.346E+02	5.425E-03	2.352E+02	3.594E-03	3.608E+02	3.129E-03	4.148E+02

Table 7. MODULE Zthj-coolant(t) FOSTER RC NETWORK VALUES

Node	NXV08H250DT1/DPT2		NXV08H300DT1		NXV08H350XT1		NXV08H400XT1/XT2	
	R, Ω	C, F	R, Ω	C, F	R, Ω	C, F	R, Ω	C, F
1	2.633E-03	1.758E-03	2.111E-03	2.205E-03	2.831E-03	1.640E-03	2.460E-03	1.887E-03
2	3.176E-02	3.152E-03	2.478E-02	4.036E-03	3.473E-02	2.913E-03	2.987E-02	3.352E-03
3	4.527E-02	4.754E-02	3.522E-02	6.119E-02	3.764E-02	5.735E-02	3.270E-02	6.601E-02
4	5.982E-01	7.776E-02	5.162E-01	9.065E-02	4.790E-01	9.773E-02	4.162E-01	1.125E-01
5	2.702E-01	2.217E+00	2.616E-01	2.266E+00	1.882E-01	3.144E+00	1.635E-01	3.619E+00
6	2.090E-02	6.087E+01	2.008E-02	6.485E+01	1.292E-02	1.022E+02	1.123E-02	1.177E+02

Switching energy can be determined from 2-pulse testing or simulation. With the simulation circuits shown in Figures 9–11, we have been able to match switching energy measurements made in our applications laboratory for the NXV08H400XT1 and have extended those results to the full line of modules based on simulation (see Tables 9 & 10).

For example, a range of gate resistance values and dc link voltages have been tested and the collected waveforms have been used to validate the simulation circuit. In Figures 13 and 14, simulation results for the turn-off and turn-on events are shown for NXV08H400XT1, for R_g external values of 5, 15, and 30 Ohms. This demonstrates the impact on turn-on and turn-off losses as well as the transient overshoot voltage on the drain due to stray inductance coupling with the resulting di/dt of the drain current.

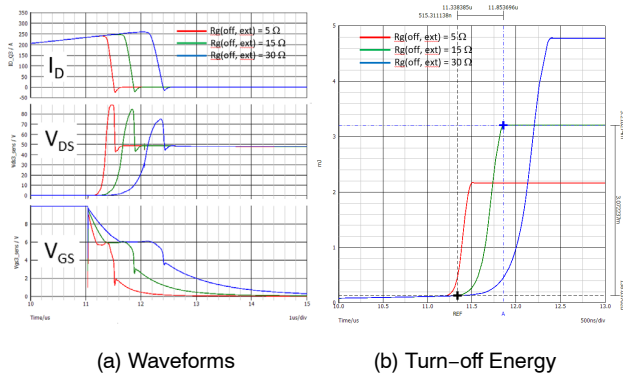


Figure 13. Simulated Turn-Off Switching Waveforms and Energy for Range of R_{g(off, ext)}, 250 A per Die

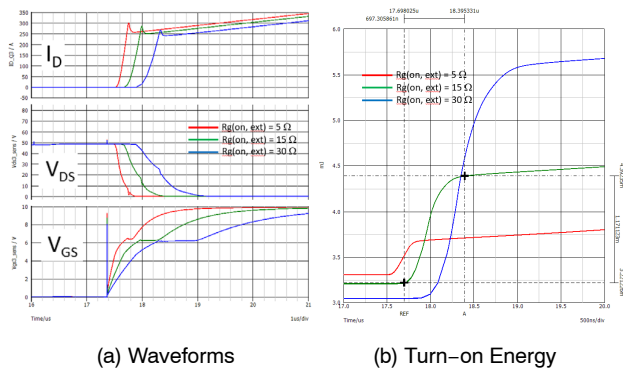


Figure 14. Simulated Turn-On Switching Waveforms and Energy for Range of R_{g(on, ext)}, 250 A per Die

By exercising the SIMetrix (or Spice) simulations, the user can develop enough loss information to accurately perform system simulations of any given operating point of the BSG/ISG system. The module losses are accurately captured by temperature-dependent values of R_{DS(on)} and operating condition-dependent switching energy. Examples of this information are given in Figure 15, again for NXV08H400XT1. Coupled with the thermal impedance characteristic, this information is sufficient to compute

conduction and switching losses and resulting die temperatures for operating conditions of interest. As mentioned above, an Excel-based system analysis tool is used to determine these quantities. An example of continuous power operation is given for the following conditions:

- R_{g(on)} = R_{g(off)} = 15 Ω
- Switching Frequency f_{sw} = 16 kHz
- Fundamental Frequency f₁ = 200 Hz
- Lockout Time = 500 ns
- V_{dc} = 48 V
- I_{phase} = 650 Arms
- T_{coolant} = 65°C

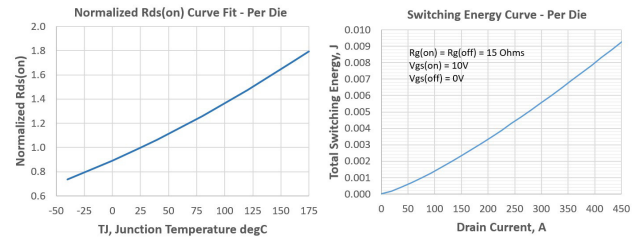


Figure 15. System Simulation Loss Component Inputs – NXV08H400XT1

Figure 16 shows the output of the analysis – die temperature and losses. The analysis is run for ~3.5 seconds of simulated time to obtain to steady state temperatures. The time necessary to achieve steady state can be observed from the thermal impedance curve in Figure 12.

Figure 16 shows the full progression of the MOSFET junction temperature, which reaches approximately 95°C, and also a zoomed in view of the temperature ripple that occurs at the fundamental frequency of 200 Hz.

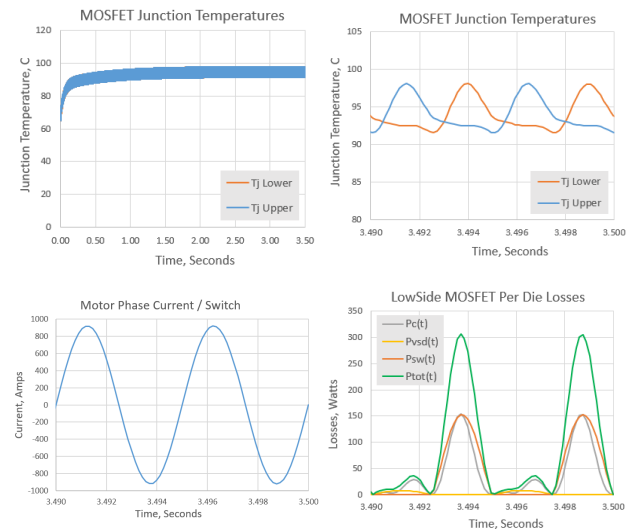


Figure 16. System Simulation Output Variables – NXV08H400XT1

The breakdown in losses is shown for the low side MOSFET, between conduction, switching, body diode, and total. As is known, the body diode only conducts during the so-called dead-time or lockout time between the high and low side FET conduction periods, thus contributing a relatively modest amount of loss to the total.

Table 8 shows a summary of the peak and average conditions experienced during this continuous power operation.

Table 8. SUMMARY STATISTICS FROM SYSTEM ANALYSIS

<i>Computed from Time Domain Results (HS&LS assumed Symmetric)</i>		
Tj(pk)	98.1	Peak junction temperature
Tj(avg)	94.0	Average junction temperature
Pc(pk)	153.9	W, peak conduction loss (per die)
Pc(avg)	40.6	W, average conduction loss (per die)
Ps(pk)	152.3	W, peak switching loss (per die)
Ps(avg)	44.7	W, average switching loss (per die)
Pdiode(pk)	8.09	W, peak Vf loss in lockout time (per die)
Pdiode(avg)	2.55	W, avg Vf loss in lockout time (per die)
Ptot(pk)	305.8	W, peak total loss (per die)
Ptot(avg)	87.9	W, average total loss (per die)
Rth	0.656	C/W, computed from RC network (1 die)

Similarly, this analysis approach can be used to examine other operating modes of the BSG/ISG, such as hill hold or engine cranking. For example, Figure 4 above introduced a sample engine cranking RMS current profile, and Figure 17 provides a detailed time-based equivalent of this phase current (first 0.5 seconds only).

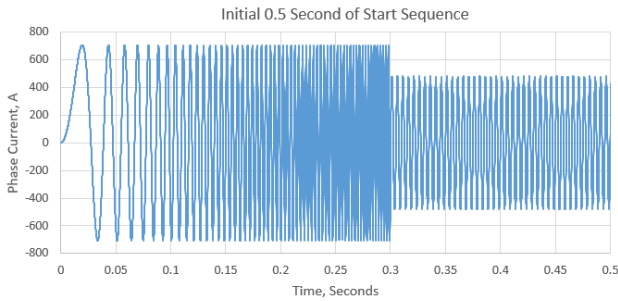


Figure 17. Example Engine Cranking Current Profile

For this condition, we assume that the initial junction temperature is elevated to 110°C. Other conditions described for the continuous power operation above still apply. One can observe in Figure 18 the phase current starting from stall and accelerating to the starting speed of 200 Hz. An initial burst of 500 Arms for 300 msec followed by 340 Arms for an additional 2 seconds is given.

From the analysis output shown in Figures 18 and 19, we can see the development of losses and junction temperature in response to the engine cranking current profile.

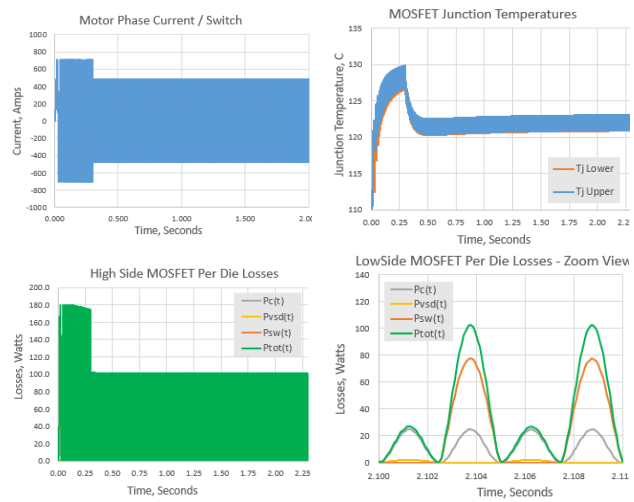


Figure 18. Total Time Engine Cranking Results

In Figure 18, we see the full profile of high side MOSFET loss, and then a “zoomed in” view of the low side MOSFET loss near the end of the starting profile.

In Figure 19 we examine the initial startup transient where the motor starts from zero speed and ramps to the starting rpm in response to the motor torque. One can see the 500 Arms current developing from 0 Hz to near 200 Hz at 0.1 seconds. Due to the low initial frequency, larger temperature pulses are observed.

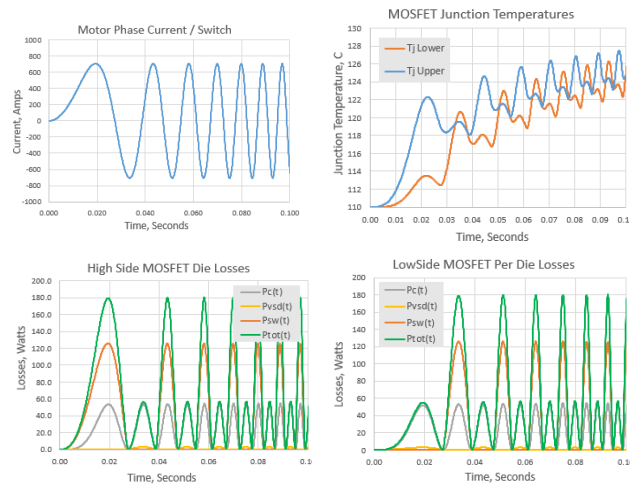


Figure 19. Initial 100 ms of Engine Cranking Results

The above two examples of system analysis are provided for continuous operation and for the engine cranking operation of the NXV08H400XT1 module as a means of illustrating the strong performance of the new onsemi high current dual half bridge modules. With basic performance information relating to conduction losses, switching losses,

and thermal impedance the system analyst can quickly evaluate the suitability of the modules for their application.

Thermal impedance characteristics are given for all modules in Tables 3 and 4 (junction-to-case) and Tables 6 and 7 (example junction-to-coolant) as Foster and Cauer RC networks. The normalized $R_{DS(on)}$ and total switching loss curves shown in Figure 15 for the NXV08H400XT1 can be generated from polynomial expressions for each of the six modules discussed in this application note.

To model $R_{DS(on)}$ as a function of temperature, the user can employ the information in Table 9 below in conjunction with the following equations:

$$R_{DS(on)}(\text{normalized}) = a \cdot T_J^2 + b \cdot T_J + c \quad (\text{eq. 1})$$

$$R_{DS(on)}(T_J) = R_{DS(on)}(25C) \cdot R_{DS(on)}(\text{normalized}) \quad (\text{eq. 2})$$

Note that the data in Table 9 is for each die in the module. The data sheet lists different values for Q1 and Q2 (high side die) versus Q3 and Q3 (low side die). As indicated in the data sheets, this is due to the kelvin sense points used to measure $R_{DS(on)}$ at final test. From the perspective of determining die temperature and losses, the lower value of these (the low side die) is more appropriate to use because it is a closer representation of the actual die on-resistance.

Table 9. $R_{DS(on)}$ (PER DIE) MODELING INFORMATION FOR MODULES

Part Number NXV08H...	$R_{DS(on)}$ (25C), mΩ		a	b	c
	Typ	Max			
250DT1	0.549	0.762	3.1705e-6	1.70e-3	0.887
250DPT2	0.56	0.71	3.1705e-6	1.70e-3	0.887
300DT1	0.46	0.58	6.0667e-6	4.1057e-3	0.891
350XT1	0.549	0.762	3.1705e-6	1.70e-3	0.887
400XT1	0.46	0.58	6.0667e-6	4.1057e-3	0.891
400XT2	0.46	0.58	6.0667e-6	4.1057e-3	0.891

In a similar manner, the switching losses for each model can be simply characterized by a power law representing the curve as shown previously in Figure 15. The equation below relates drain current and DC voltage to the total switching losses, for a range of DC voltage from ~36 V to ~56 V. V_{ref} for all cases is 48 V. The values for k, n, and x for the **onsemi** modules are given in Table 10.

$$E_{sw}(I_D, V_{DC}) = k \cdot I_D^n \cdot \left(\frac{V_{DC}}{V_{ref}}\right)^x \quad (\text{eq. 3})$$

Table 10. TOTAL SWITCHING ENERGY (PER DIE) MODELING INFORMATION FOR MODULES

Part Number NXV08H ...	$R_{g(on/off)} = 15/15 \Omega$		$R_{g(on/off)} = 30/15 \Omega$		x
	k	n	k	n	
250DT1 250DPT2 350XT1	4.26e-6	1.258	9.95e-6	1.175	1.185
300DT1 400XT1 400XT2	3.00e-6	1.296	7.22e-6	1.208	1.798

GATE DRIVER RECOMMENDATIONS

onsemi provides solutions for 48 V BSG/ISG applications beyond the boundary of the power modules described in this application note, as can be seen from our website www.onsemi.com, and the 48 V system block diagram shown in Figure 20. Of particular interest for this application note are the gate drivers that are available from **onsemi**.

Two series of gate driver IC’s available from **onsemi** are particularly useful for driving the NVX08H-series of power modules: the FAD3151/3171 [10] and NCV5707B [11]. These drivers provide high current and voltage capability suitable to drive the large die MOSFETs in the modules, and desaturation detection and soft turn off features to handle overcurrent or short circuit current conditions.

If the user’s system is required to protect against short circuit conditions, it is necessary to manage well the detection and soft turn off operation in order to achieve a fault-tolerant design.

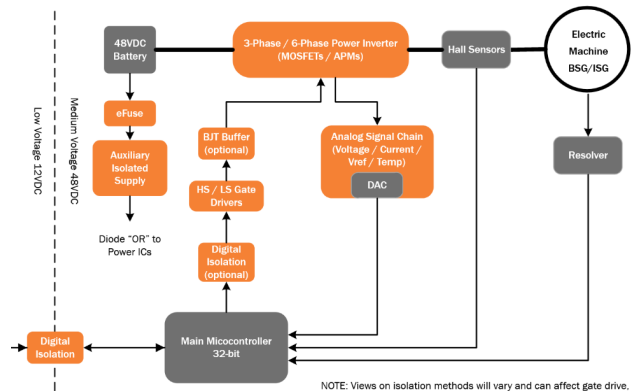


Figure 20. 48 V BSG/ISG Application Block Diagram

FAD3151/3171

The FAD3151 and FAD3171 are single channel floating automotive gate drivers suitable for driving high-speed power MOSFETs up to 110 V. Designed in a SOI technology, the drivers are ideal for applications that require noise immunity against severe negative transients and ground offset up to -80 V. They operate as a pair of ICs as shown in the application schematic in Figure 21.

The FAD3151/3171 drivers have an integrated desaturation detection to protect the power switches during short circuit and over current conditions. The drivers are also equipped with a soft shutdown feature, which initiates a soft shutdown of driver outputs upon desat detection, thus preventing possible overvoltage across power MOSFETs during a heavy-load condition.

The FAD3151/3171 drivers are equipped with bidirectional fault reporting pin that can generate a fault output during desat and under-voltage lockout (UVLO) condition. The bidirectional nature of the fault-reporting pin allows the driver to respond to external fault commands, thereby facilitating fault communication across the system. In addition, the FAD3171 has an integrated charge pump to support 100% duty cycle operation of high side MOSFETs.

The gate driver has a desaturation detection circuit that monitors the drain to source voltage V_{DS} of the power MOSFET through the desaturation detection pin. This circuit consists of:

- An internal current source that provides a continuous current toward the power stage to monitor the V_{DS} voltage. The desat current source (I_{DESAT}) is supplied from the VB pin and is continuously active as soon as the VDD is higher than the UVLOVDD+, independent of the status of the input logic.
- An internal comparator that compares the voltage at the desat pin (V_{DESAT}) with the defined desat threshold ($V_{DESAT,TH}$) of 3 V (typ). When V_{DESAT} exceeds $V_{DESAT,TH}$, the comparator simultaneously turns off the output ‘slowly’ and triggers a fault condition by pulling down the fault pin internally.

As shown in application schematic in Figure 21, the desat diode D1, resistor R1, blanking capacitor CBL, and P-channel JFET P1 are the minimum external components required to operate the desaturation protection scheme. The driver needs an external pull-down transistor P1 to discharge I_{DESAT} and CBL as soon as the driver output turns off.

Otherwise, the blanking capacitor will continue to charge up and eventually trigger desat. The presence of a normally on P1 also enhances noise immunity of the desat blanking capacitor against false triggering during the turn-on event of complementary power switch. The external desat components can be modified to adjust the blanking time and the desat detection threshold for a given application.

If the power switch is turned off rapidly during a heavy load condition, the high currents may generate a voltage overshoot across the power switch that could potentially damage it. In order to protect the devices, the driver has a soft shutdown feature, which activates upon desat detection. The output is then driven low through a large turn-off resistance (RSOFT) which provides a significantly higher resistance path for the gate capacitance to discharge than during the regular turn-off process. As a result, the possibility of an abrupt overvoltage spike on the power switches is reduced.

When the voltage at the desaturation pin exceeds the defined desat threshold, following protection sequence is performed:

- The gate driver initiates a soft shutdown. The driver will provide a high resistance path through an internal resistor for gate capacitance to discharge slowly as shown in Figure 22.
- The fall rate of HO is determined by the time constant of the RC discharge path. The driver also triggers an internal fault and pulls down the fault pin for the period equivalent to Fault Locking duration (typ. 550 μ s).

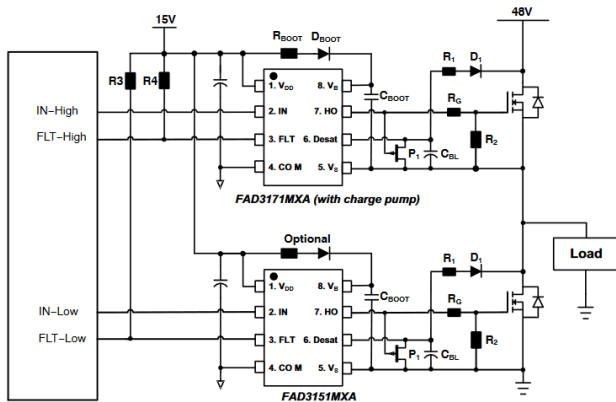


Figure 21. Application Diagram for FAD3151/3171 Driver IC

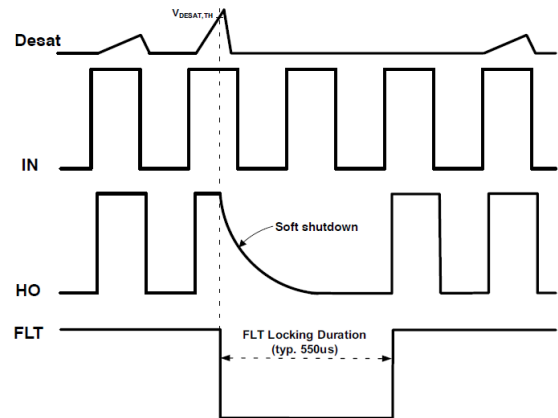


Figure 22. FAD3151/3171 Desaturation Detection and Soft Shutdown

Additional details regarding the operation of the FAD3151/3171 are given in [10]. Here we simply highlight

the necessary desat detection and soft turn-off capability of this IC to enable short circuit protection in the NXV08H-series of modules.

NCV5707B

The automotive qualified NCV5707B is an 8-pin SOIC part in a series of high current, high performance standalone drivers for high power applications that include the BSG/ISG modules. The devices offer a cost-effective solution by eliminating the need for an external output buffer. Protection features include accurate Undervoltage Lockout (UVLO), desaturation protection (DESAT) and active open drain FAULT output.

The drivers also feature an accurate 5.0 V output. The drivers are designed to accommodate a wide voltage range of bias supplies. The NCV5707B accommodates bipolar voltages.

A companion part (NCV5707A) also includes Active Miller Clamp and separate high and low (VOH and VOL) driver outputs for system design convenience (NCx5707C).

To emphasize the desat detection and soft turn-off features of the IC which are necessary to protect against short circuit conditions in the NXV08H-series of modules, the following information about the NCV5707B is provided from [11].

The desaturation detection feature monitors V_{DS} in the turned-on state. When the MOSFET is fully turned on, it operates in the $R_{DS(on)}$ region. V_{DS} is usually low because it is $R_{DS(on)} \cdot I_D$, and $R_{DS(on)}$ for these parts is below 1 mΩ, well below 3 V in the NXV08H-series modules. It could indicate an overcurrent or similar stress event on the MOSFET if the drain-source voltage rises above the saturation voltage, after the MOSFET is fully turned on. Therefore, the DESAT protection circuit compares the drain-source voltage with a voltage level $V_{DESAT-THR}$ to check if the MOSFET is experiencing extreme levels of I_D . It will activate FLT output and shut down driver output (thus turn off the MOSFET), if the drain-source voltage rises above the $V_{DESAT-THR}$. This protection works on every turn on phase of the MOSFET switching period.

To prevent the voltage overshoot damage caused by turning off the MOSFET, the NCV5707B driver is equipped with a “Soft Turn Off” (STO) function. This function is activated when the DESAT protection is activated and reduces the turn off voltage overshoot by adding a large internal turn off resistance in series with the external $Rg(off)$.

At the beginning of MOSFET turn-on, the drain-source voltage is much higher than the voltage which is present after the MOSFET is fully turned on. It may take ~1 μs between the start of the MOSFET turn-on and the moment when the drain-source voltage falls to the fully on level.

Therefore, the comparison is delayed by a configurable time period (so-called blanking time) to prevent false triggering of the DESAT protection before the MOSFET drain-source voltage falls below the saturation level. Blanking time is set by the value of the capacitor C_{BLANK} .

The exact principle of operation of DESAT protection is described with reference to Figure 23. At the turned-off output state of the driver, the DESAT pin is shorted to ground via the discharging transistor (Q_{DIS}). Therefore, the inverting input holds the comparator output at low level.

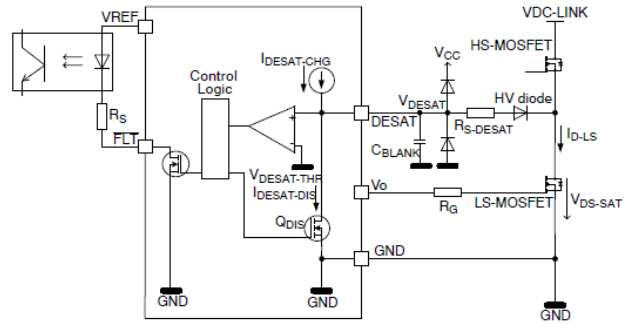


Figure 23. NCV5707B Desaturation Protection Schematic

At the turned-on output state of the driver, the current $I_{DESAT-CHG}$ from current source starts to flow to the blanking capacitor C_{BLANK} , connected to DESAT pin.

An appropriate value of this capacitor has to be selected to ensure that the DESAT pin voltage does not rise above the threshold level $V_{DESAT-THR}$ before the MOSFET fully turns on.

The blanking time is given by following expression. According to this expression, a 47 pF C_{BLANK} will provide a blanking time of $47 \text{ pF} \cdot 6.5 \text{ V} / 0.25 \text{ mA} = 1.22 \text{ μs}$.

$$t_{BLANK} = C_{BLANK} \cdot \frac{V_{DESAT-THR}}{I_{DESAT-CHG}} \quad (\text{eq. 4})$$

After the MOSFET is fully turned-on, the $I_{DESAT-CHG}$ flows through the DESAT pin to the series resistor $R_{S-DESAT}$ and through the high voltage diode and then through the drain and source. Care must be taken to select the resistor $R_{S-DESAT}$ value so that the sum of the saturation voltage, drop on the HV diode and drop on the $R_{S-DESAT}$ caused by current $I_{DESAT-CHG}$ flowing from DESAT source current is smaller than the DESAT threshold voltage. Following expression can be used for the DESAT threshold voltage:

$$V_{DESAT-THR} > R_{S-DESAT} \cdot I_{DESAT-CHG} + V_{F-HVdiode} + V_{DS}$$

where V_{DS} is the drain-source voltage under high- or short-circuit current levels.

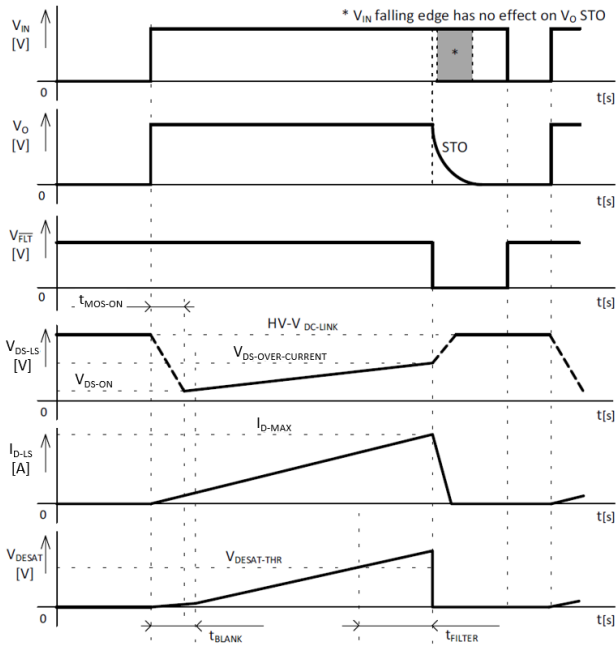


Figure 24. NCV5707B Desaturation Protection Schematic

It is important that the high voltage diode is rated at 80 V for the NXV08H-series modules, with a safety margin if desired by the end user. The typical waveforms for the MOSFET overcurrent condition are outlined in Figure 24.

MECHANICAL MOUNTING CONSIDERATIONS

The dual half-bridge APM module is a compact semiconductor power module with low power-consumption and high reliability. Target applications are inverter motor drives for 48 V MHEVs. To achieve the high performance and long life needed for this demanding application, proper mounting with good thermal performance and low mechanical stress is needed. In this section, we provide mounting guidance for this series of modules.

Figure 25 shows the two general methods of assembly for typical transfer molded power modules. Assembly is commonly done using method 1 or method 2 based on the customer’s preference. This application note is intended to provide recommendations for proper handling, assembly of the package and potential rework in conjunction with industry standards. We also outline appropriate thermal interface material (TIM) application and heat sink mounting as well as soldering procedures to ensure a reliable printed circuit board (PCB) connection. Recommendations in this note are based on simulation and experimental results from laboratory and field tests.

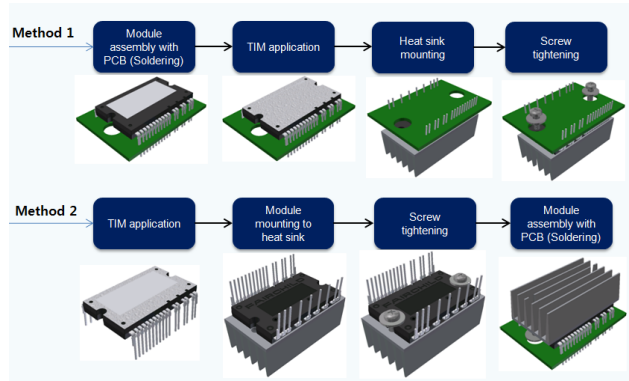


Figure 25. General Assembly Methods

For high power modules, the power terminals can be connected directly to the busbar through a welding process, such as resistive welding, according to the customer’s preferred technique. It is preferred to connect the power terminals directly to the bus bar to avoid bringing excessively high current onto a PCB, since this would require special PCB construction and materials to handle the current efficiently.

Package Surface Specification

The measurement area for the warpage of the package surface is specified by the package center and the four outside corners, as shown in Figure 26. Warpage for the modules is as specified in Table 11. When assembled with recommended screws and torque, the surface will be flattened and the thermal compound between module and heatsink will spread out and fill the microscopic air gaps between the two contact partners, finally ensuring full thermal contact. Warpage is guaranteed to be concave up (so-called “smile shape”) such that the screw torque will flatten the module onto the heatsink surface.

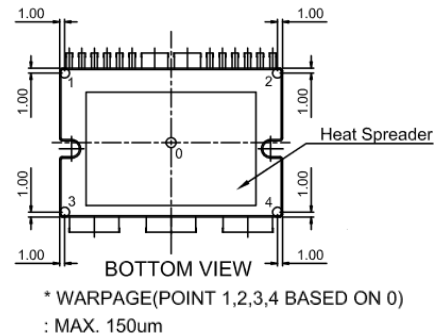


Figure 26. Determination of Package Warpage

Table 11. SPECIFICATION OF THE APM PACKAGE WARPAGE

Module	Min	Typ	Max
NXV08H250DT1 NXV08H250DPT2 NXV08H300DT1 NXV08H350XT1 NXV08H400XT1 NXV08H400XT2	+35 μm	+55 μm	+150 μm

Heat Sink Surface Specification

The thermal performance of a module is influenced by the quality of the surface contact to the heat sink. To maximize the heat transfer it is required to maintain a high quality heat sink surface, that is, surface flatness and roughness must be properly specified and controlled when manufacturing the heat sink. To obtain best performance, the specifications given in Table 12 and Figure 27 should be followed in the heatsink design and manufacture. Additionally, the desired heat flow from heat sink to ambient for the customer’s application conditions must be achieved. The surface of the heat sink must be clean and free of particles during assembly.

Table 12. HEAT SINK SURFACE REQUIREMENTS

Flatness of Heat Sink	-50 ~ 100 (μm)
Geometrical Surface Roughness (Rz)	≤ 10 (μm) to DIN EN ISO 4287

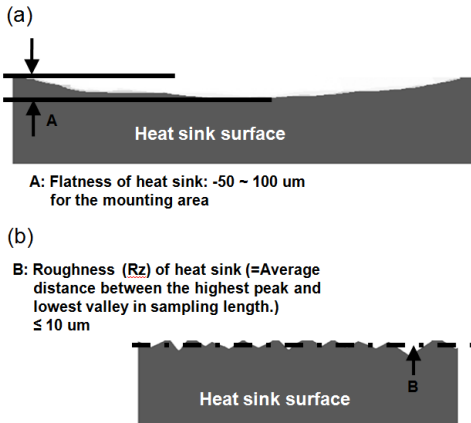


Figure 27. Determination of Package Warpage

Assembly Sequences

The assembly process can be done in two ways: either mounting the module onto the heat sink first and then proceeding to soldering the signal pins; or soldering the module on the PCB first followed by mounting on the heat sink.

Module mounting to the heat sink first, then soldering to the board and/or welding power terminals.

When the module is mounted onto the heat sink before PCB mounting, a process flow as illustrated in Figure 28 is recommended. First, apply TIM on the surface of the module or heat sink and place the module on the heat sink (a). Tighten the screws down to heat sink (b). Then the module with the heat sink is placed onto the PCB (c). Finally, the solder joint between signal pins and PCB is formed (wave soldering process or manual soldering)

Manual soldering, wave soldering, and selective soldering are possible techniques to assemble the module onto the PCB. For the power terminals, a laser or resistive welding process can be used to connect the power terminals directly to the bus bar. With manual soldering, both bottom side and top side soldering is available. Wave soldering systems consist typically of solder fluxing, preheating zone, solder wave and the cooling zone. As the board enters the conveyerized process, solder flux is sprayed or foamed onto the modules.

Then it moves to the preheating zone, normally done by convection, where the flux is activated. The assembly then moves to wave soldering. The assembly is then slowly cooled down.

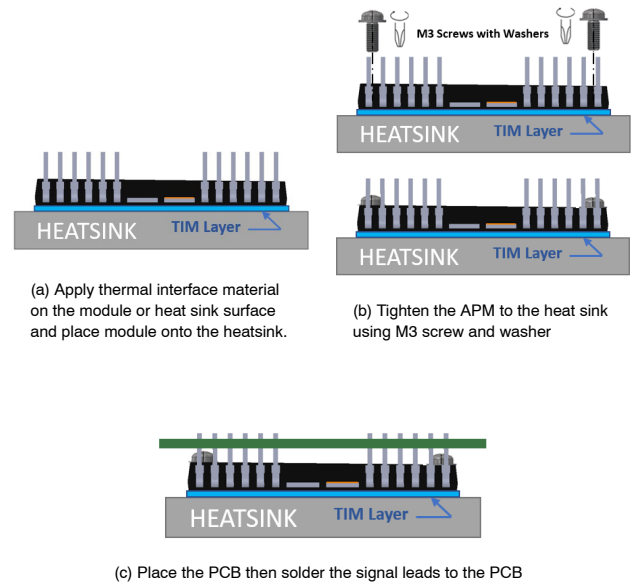


Figure 28. Process Flow of Soldering APM Package (When Heat Sink Mounting First)

Soldering to the PCB, then mounting to the heat sink

If the module is assembled with the PCB first and heat sink mounting is conducted second, the process flow described in Figure 29 is recommended. First, the module is place on

the PCB (a). Then, soldering signal leads to the PCB is done (b). After PCB assembly is complete, thermal interface material is applied on the surface of the module or heat sink (c). The module/PCB assembly is then placed onto the heat sink and fixed to the heat sink via screws (d).

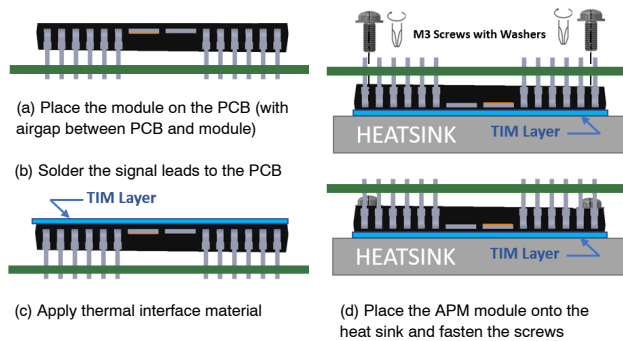


Figure 29. Process Flow of Soldering APM Package (When PCB Mounting First)

System considerations (Optional per designs)

After the module is assembled to the PCB and the heat sink as described above, the overall structural integrity needs to be considered in terms of mechanical stress to any of the system components. In case the PCB is large and heavy with other components assembled to it, there is some risk the PCB can bend, creating mechanical stress to the module and the PCB. In addition, when multiple modules are applied to the same PCB, height tolerances between modules can result in mechanical stresses to the board and modules. Figure 30 illustrates one method to prevent PCB bending and stress by using spacers between the PCB and heat sink. Various types of spacers could be added on the heat sink, to prevent any possible movement of the PCB.

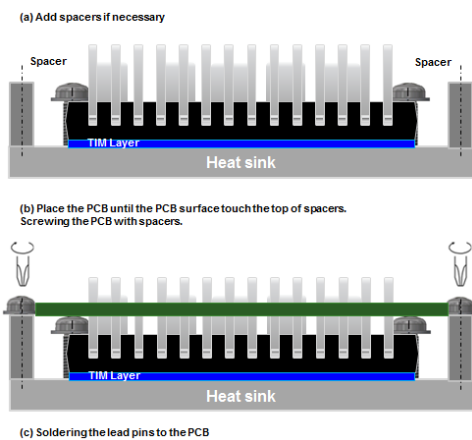


Figure 30. Robust Assembly Method of APM Package to Reduce Stresses from PCB Bending

Mounting with the spacers

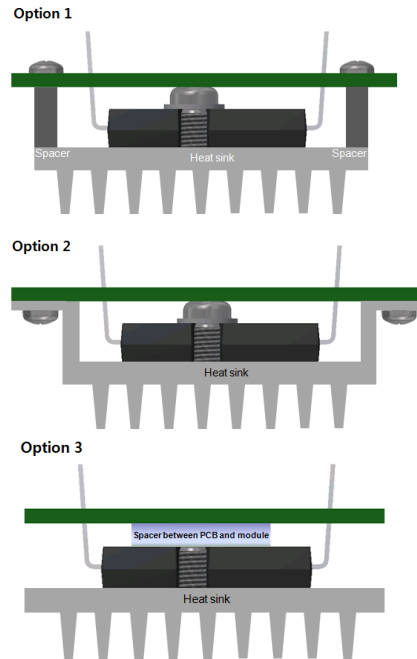


Figure 31. Examples of the Spacer Type

Figure 31 shows examples of possible spacer types. Option 1 shows individual spacers between the heat sink and PCB concentric with the PCB mounting screws. Option 2 illustrates a heatsink with integrated standoffs to provide the spacing. Option 3 shows a separate spacer situated between the module and the PCB.

Thermal Interface Materials (TIM) for Electronics Cooling

Since the contact surfaces are not perfectly flat, multiple air gaps can form between two solid contact surfaces. Air is a poor heat conductor preventing the heat transfer and limiting the effective contact area. Thermal Interface Materials (TIM) need to be applied between the heat sink and the module surface to fill any air gaps and to achieve a low thermal resistance. The following are general considerations when choosing the material for the application. Besides its thermal conductivity, handling and rework performance may be important factors while selecting the proper TIM.

- High thermal conductivity
- Ease of distribution (spreading) with low contact pressure
- Minimal thickness (electrical isolation not needed)
- Degradation of characteristics over time
- Environmental impact
- Ease in handling during application or removal

Although thermal interface materials with improved performance are available nowadays, the most commonly used in the industry is still thermal grease.

Users should make sure that the TIM is applied with desired thickness and spread evenly across the interface, based on the TIM datasheet and desired thermal resistance. The viscosity of the TIM will impact the thickness of the TIM after mounting the module. Only a small amount of compound is required to fill the gap between the contacting surfaces. One of the recommended interface materials is Electrolube® HTCP (Heat Transfer Compound Plus) thermal grease [12]. HTCP is a non-curing, non-silicone heat transfer paste suitable for the application where silicones are prohibited, thus avoiding issues with silicone and low molecular weight siloxane migration. It is RoHS-2 compliant.

As an alternative, high thermal conductivity graphite sheets provide improved reliability, high thermal performance, and lower overall costs due to a simplified assembly process. However, the thermal resistance depends on the thickness of the graphite sheet. Hence, the thickness and thermal conductivity should be carefully reviewed before the selection. It is recommended to contact your local **onsemi** representative for more information.

Manual TIM Application

Thermal grease can be applied to the heat sink or the module back surface using a rubber roller or spatula, by screen printing or auto dispenser. A rubber roller, as shown in Figure 32, is an easy and fast method for applying thermal grease. Since the thermal grease has the lowest thermal conductivity in the thermal path, a layer as thin as possible is necessary to keep the overall thermal resistance low. Recommended thickness of printing layer is uniform dispense of a minimum 150 µm. The thermal grease thickness can be checked using thickness gauges, such as wet film combs or wet film wheels. Since manual control of printing pressure and speed can be learned by experience, training is needed to achieve a technique for good quality printing in the application.

TIM Application by Manual Screen Printer

Stencil/screen printing can be utilized for the application of thermal paste. It allows a fast, clean and easy handling of spreadable TIMs. They can be applied to the substrate area, leaving out other parts of the module package using specifically designed stencils. An optimization of the screen mask pattern and thickness is required to achieve a good quality of the print and finally and optimum contact.

Figure 33 shows an example of thermal paste application process using a manual screen print.

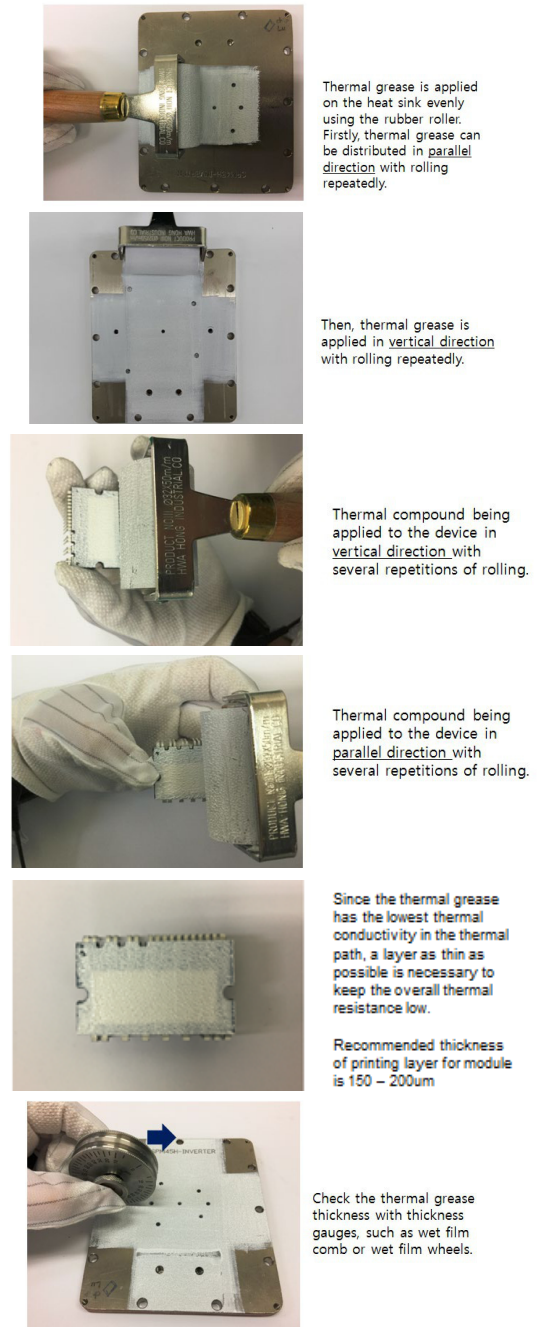
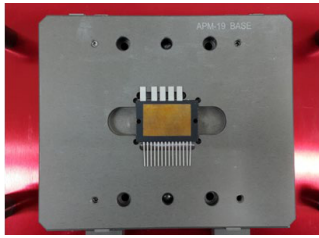
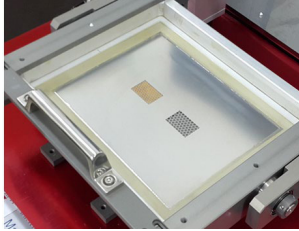


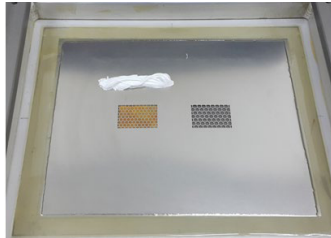
Figure 32. Example of Thermal Grease Application Using a Rubber Roller



Place the module on the mounting jig. Ensure the DBC area is clean. (Sample is APM 19)



Aligning and positioning of the screen mask to the module DBC area



Dispense the thermal interface material on the screen mask



Place the squeegee or spatula behind the TIM and tilt down it to have 45° angle around. Apply a certain pressure and draw the squeegee downwards slowly.

Maintaining the constant printing pressure and speed make possible to achieve uniform pattern of printing layer.

Figure 33. Example (APM19 Package) of Thermal Paste Application Using a Manual Screen Print

Fully automated screen printing is recommended in mass production. It yields a high quality printing layer with high accuracy and repeatability.

Considerations on Screw Tightening

APM packages should be secured on the heat sink via two M3 screws. The location of the screw holes is illustrated in Figure 34. Table 13 shows the screw specification and Table 14 is showing the recommended torque ranges for the APM19 and APM21 package. Contact pressure and mounting torque may affect the thermal performance. The thermal resistance specified can be achieved with the minimum resistance specified torque in the Table 14. Electric screwdrivers can tighten the screws with the specified torque. Figure 35 shows SEMS (pre-assembled washers and screw) which is a recommended screw type.

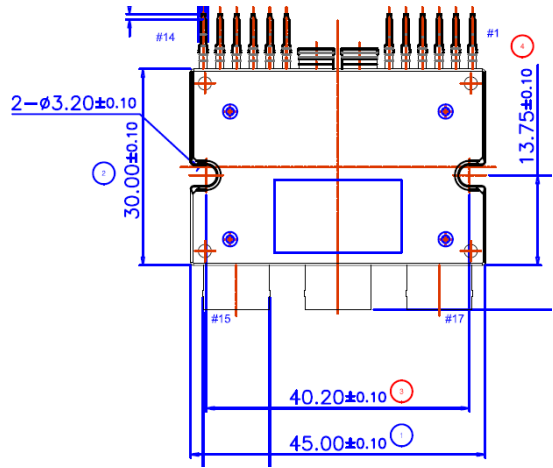


Figure 34. Dimension of Screw Clamping Zone (mm)

Table 13. SCREW AND WASHER INFORMATION

Parameter	Description
Mounting Screw	Metric M3 Screw
Spring Washer	D (Nominal) = ø5.5 (mm), t = 1.2
Plain Washer	D (Nominal) = ø7.0 (mm), t = 0.5 (mm)
Recommended thread engagement for screws with property class 4.8 to 6.8 for different materials	

In case of the usage of special screw without the washer, such as using TAP TITE screw without washer, the diameter of the screw head is important. If the screw mount torque is over 0.8 N.m, it is recommended to use the screw with a minimum 6.2 mm diameter screw head.

Table 14. MOUNTING TORQUE SPECIFICATION FOR (M3)

Parameter	Unit	Min.	Max.
Pre-Torque	[N·m]	0.2	0.4
	[kgf·cm]	2.0	4.1
Final Torque	[N·m]	0.6	1.4
	[kgf·cm]	6.1	14.3
Generally, pre-torque is 20–30% of the final torque			



Figure 35. SEMS (Pre-assembled Washers and Screw, Spring Washer ø 5.5 and Plain Washer ø 7.0)

Thermal Performance under Various Mounting Torque

Since the module surface and heat sink are not perfectly flat, contact pressure and mounting torque can affect thermal performance. According to the results shown in Figure 36 (typical for APM packages), thermal resistance values (R_{thjc}) achieve stable values at torque levels ranging between 5~7 (kgf-cm) with APM packages with M3 screws.

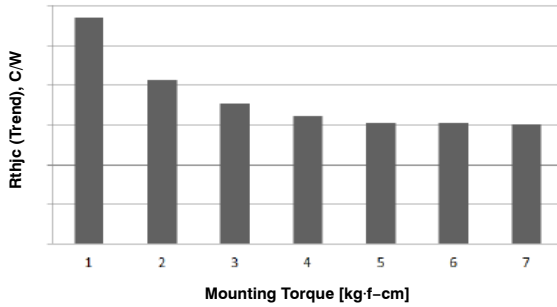


Figure 36. Rthjc under Various Mounting

Screw Tightening Method

Screw tightening can be done in various ways. Figure 37 describes one recommended method for fastening the module to the heat sink. Fasten two screws with final torque simultaneously to prevent tilting or rising of top side of module during fastening.

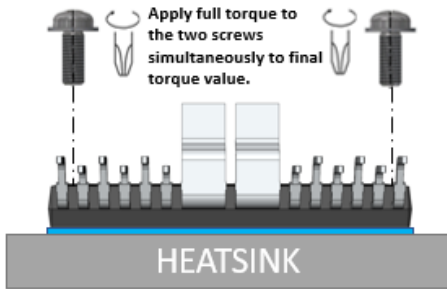


Figure 37. Illustration of Screw Clamping with Heat Sink

Alternatively, Figure 38 shows another recommended method to tighten the screws. Fasten the first screw with pre-torque to prevent one side tilting or rising of the module (Step 1). Then insert the second screw to the other side with same pre-torque (Step 2). The pre-screwing torque is set to 20~30 % of final torque rating. After that, apply full final torque to the first screw (Step 3). Finally, apply full torque to the second screw for proper mounting to the heat sink (Step 4). An insufficient tightening torque may cause an increased thermal resistance or loosening of the screws during operation.

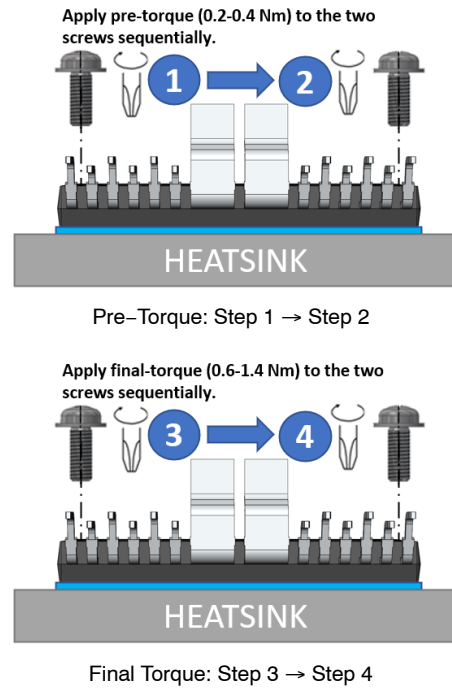


Figure 38. Illustration of Screw Clamping with Heat Sink

Notes on Assembly:

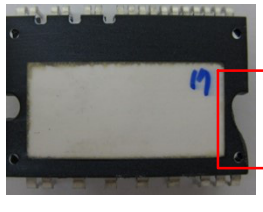
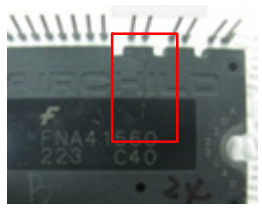
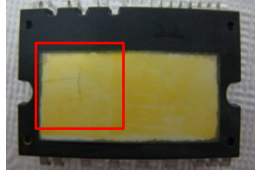
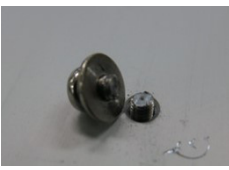
- Avoid applying over torque when mounting screws. Excessive fastening force may cause damage to the semiconductor devices, the package or its isolation, as well as damage to the screws or heat-sink.
- Uneven mounting can cause the ceramic substrate to be damaged. A smooth surface free of burrs and protrusions or indentations is required. No foreign materials except thermal interface materials are allowed between surface of the module and the heat sink.
- The mounting area should be treated as a functional layer. Do not touch the mounting area of the heat sink and the substrate of the module.

Potential Failure Modes

The following are possible root causes of mounting failures which should be avoided during the mounting process. Table 15 lists representative examples of mounting failure mode.

- Excessive torque is applied without pre-torque
- Misalignment of screw during tightening with heat sink
- Mechanical stress by mounting height tolerances when multiple module mounted on the same PCB
- Inappropriate type of screws are used

Table 15. EXAMPLES OF MOUNTING FAILURE MODES

	
EMC broken due to excessive torque	EMC crack due to non-flat heatsink
	
Cracked ceramic substrate	Broken fasteners

Clip Mounting

As an alternative method, “Clip mounting” can be used to fasten the module to the heat sink. In such a case, the screw mount holes can be used for locating pins, while two side contact points provide vertical pressure to the module.

For this method, detailed mechanical design of clip and pressure force is required. It is recommended to contact your local **onsemi** representative for more information to validate the system design using clip mounting methodology. There is no general guidance for clip, so the customer’s design must be validated case by case for the specific clip design.

The NXV08H-series of APM modules incorporates an exposed copper exterior surface of the ceramic substrate to facilitate improved heat spreading and heat transfer. The surface of the copper layer may oxidize during manufacturing, storage, and transportation. This is not a concern for the performance of the module, and further details may be obtained in [13].

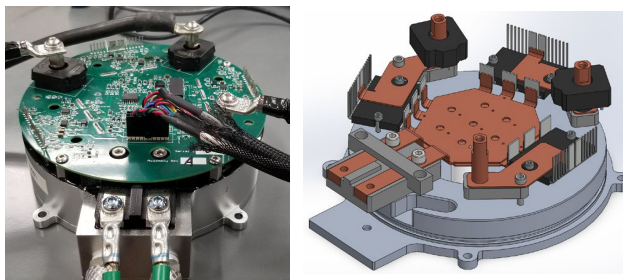


Figure 39. Photo of 25 kW BSG/ISG

REFERENCE DESIGN HARDWARE AND TEST RESULTS

A 25 kW BSG/ISG reference design was created for the purposes of testing the NXV08H-series of power modules. This design included a liquid-cooled heat sink, dc capacitor bank, dc and ac bus bar, and gate drive PCB with external interfaces to a separate controller. A photo is shown in Figure 39, along with a CAD representation of the assembly without the PCB.

A general requirements specification for this reference design was provided to the design team as shown below:

- 3-Phase Automotive Liquid Cooled Power Inverter Stage
- Input Voltage Rating (Nominal): 48 V
- Input Voltage Range: $36\text{ V} \leq V_{DC} \leq 52\text{ V}$
- Continuous Current Rating: $I_{PHASE} \leq 400\text{ Arms}$
- Peak Current Rating (30s): $I_{PHASE} \leq 700\text{ Arms}$
- Isolated Input Control and Fault Feedback Signals
- Active Over-Temp and Over-Current Protection with Auto-Shutdown
- Two Isolated Phase Current Feedback Sensors
- Coolant Temperature: $70^{\circ}\text{C} - 85^{\circ}\text{C}$

Inverter Construction

The inverter assembly is constructed in a stacked format, as shown in Figure 39, employing three of the NXV08H400XT1 modules. At the top of the stack, the PCB contains the logic and interface circuitry as well as the phase current sensors. Below the PCB are the power modules, shown with small bus sections that route the phase connections between the modules and the phase output connectors. The inverter 3-phase output connectors are located on top of three threaded posts. These posts pass through the current sensors. Next, are the main bus bar assembly which connects the input terminals, the bus capacitors and the module DC connections. Finally, the heat sink cools the power modules and the capacitor bank and provides a mounting surface for all the pieces. The internal housing of the heatsink is formed with a pin-fin structure to more effectively remove the module heat while maintaining a low pressure drop. It is constructed as a two-piece assembly, with the bottom cover connecting to the top section with threaded fasteners and an o-ring for sealing.

Output Section

The output section of the inverter consists of three half-bridge NXV08H400XT1 power modules, shown in Figure 40. As we know, the module embodies two independent half-bridge sections, having common power

connections. It can be used either as two half-bridges or, when connected in parallel, as a single half-bridge. In this application the two half-bridges are connected in parallel and the module is operated in a single half-bridge configuration. The three modules are connected to a common 48 V power bus, with each of the modules' ac outputs being connected to one of the three output phase connections.

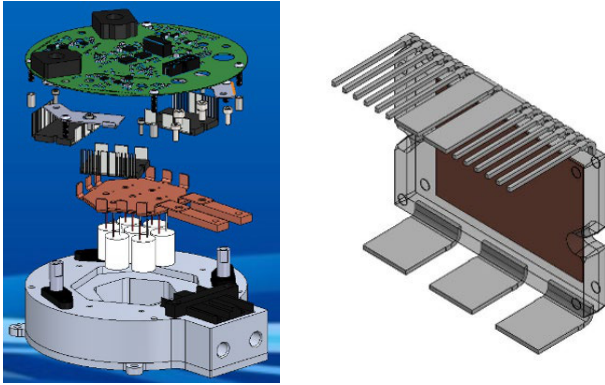


Figure 40. Stack Assembly Inverter and Module

Gate Driver Circuitry

Since this inverter was designed for use with an external system controller, cross-conduction protection is provided on-board. The FAN73832 [14] half-bridge gate driver was used to provide the dead-time function, which may be adjusted from 400 ns to 1.6 μ s. The FAN73832 operates with a single input and single output disable pin, permitting both PWM and ENABLE control signals. In this application it acts only as a logic support device. The output of the FAN73832 is connected directly to a cascaded gate drive IC, the FAN7191 [15], which is responsible for providing the drive current necessary to drive the module MOSFETs' gates.

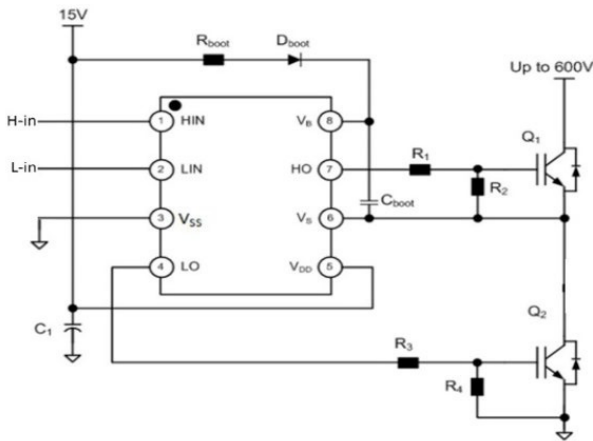


Figure 41. FAN7191 Application Circuit

The FAN7191 is capable of sourcing and sinking 4.5 amps. It has an under-voltage lockout, matched dual channel propagation delay and can tolerate up to a -9.8 V of negative level shift. The HO and LO pins are connected to the module gates through 10 Ω resistors, with each channel driving the gates of the two paralleled MOSFETs. Even though the internal devices are connected in parallel, they still have separate gate connections. An example circuit diagram of the FAN7191 is shown in Figure 41.

Bench Test Results

The inverter assembly was tested on the bench setup shown in Figure 42, under the following conditions:

- Passive RL load with L~46 μ H, R~1 m Ω per phase
- 50/50 water/glycol coolant at ~4 LPM flow rate
- 48 V < V_{DC} < 54 V
- Fundamental frequency 50 to 200 Hz
- Sine-triangle PWM switching at 10 kHz
- Dead-time (lockout) ~ 1.4 μ s
- Control by LabView via CompactRIO [16]

The system was tested with phase current up to 700 A_{RMS}. Under these conditions, the losses for the inverter stage (DC input power to ac output power) ranged up to 2.6 kW. The loss curves are shown in Figures 43 and 44 for coolant temperatures of 25°C and 65°C. The passive RL load presents a very low power factor (~2%) which is not realistic for a motor drive but which nonetheless provides the opportunity to determine the losses as a function of motor phase current. The MOSFET inverter losses have minimal sensitivity to power factor or modulation index, unlike and IGBT/diode based inverter.

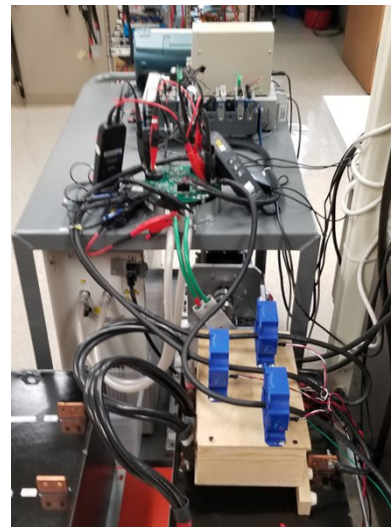


Figure 42. Photo of Test Bench Setup

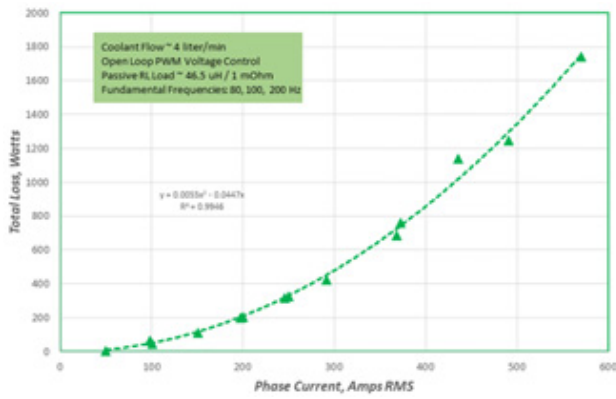


Figure 43. Inverter Loss, 25°C coolant, 48 VDC, 10 kHz Switching Frequency

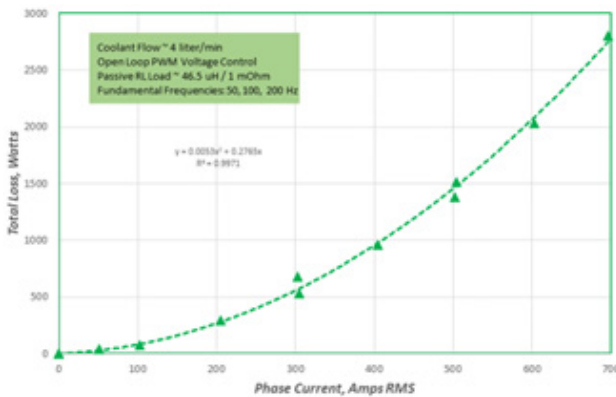
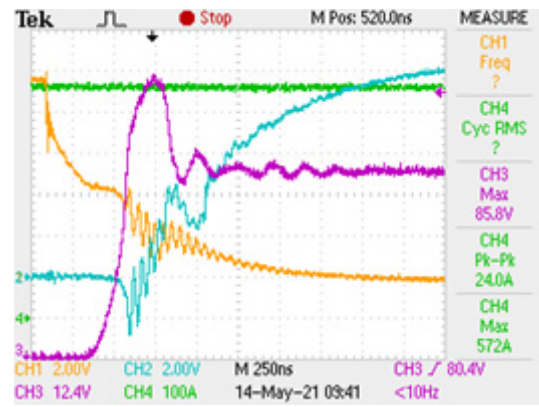
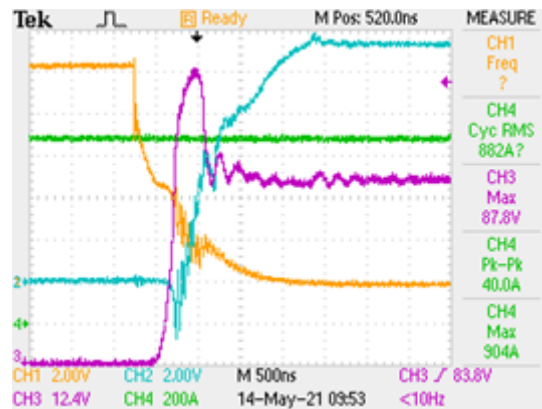


Figure 44. Inverter Loss, 65°C coolant, 54 VDC, 10 kHz Switching Frequency

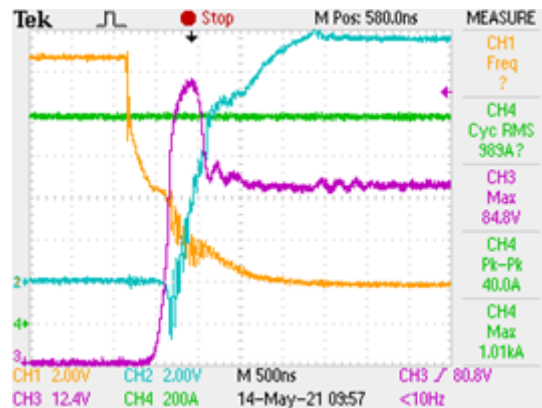
Switching waveforms for the inverter operating at peak currents of approximately 575 A, 880 A, and 990 A are shown in Figure 45. Channel 1 is V_{GS} of Q1, Channel 2 is V_{GS} of Q4, Channel 3 is V_{DS} of Q1, and Channel 4 is I_{PHASE} .



(a) 575 A



(b) 880 A



(c) 990 A

Figure 45. Switching Waveforms

REFERENCES

- [1] “Road vehicles – Supply voltage of 48 V – Electrical requirements and tests,” ISO21780.
- [2] Brian A. Welchko, et al, “IPM Synchronous Machine Drive Response to Symmetrical and Asymmetrical Short Circuit Faults,” IEEE Transactions on Energy Conversion, Vol. 18, No. 2, June 2003, pp. 291–298.
- [3] [AND90096/D](#), “Usage of SIMetrix to Study MOSFETs Thermal Behaviors on Heatsink,” March, 2021.
- [4] [AND9783/D](#), “How to Use Physical and Scalable Models with SIMetrix, OrCAD and LTSpice,” August 2018.
- [5] “OrCAD PSpice Designer,” OrCAD Cadence PCB Solutions website, <https://www.orcad.com/products/orcad-pspice-designer/overview>
- [6] “SIMetrix,” SIMetrix Technologies website, <https://www.simetrix.co.uk/products/simetrix.html>
- [7] “LTSpice,” Analog Devices website, <https://www.analog.com/en/design-center/design-to-ols-and-calculators/ltspice-simulator.html>
- [8] ANSYS Q3D Extractor, Multiphysics Parasitic Extraction & Analysis, www.ansys.com/products/electronics/ansys-dq3d-extractor.
- [9] MathWorks MATLAB, www.mathworks.com/products/matlab.html
- [10] **onsemi** Data Sheet FAD3151/3171, “110 V 2.5 A Single Channel Floating Gate Drivers with Desaturation Protection and Charge Pump”, www.onsemi.com/download/data-sheet/pdf/fad3152-mxa-d.pdf
- [11] **onsemi** Data Sheet NVV5707B, “High Current IGBT/MOSFET Gate Drivers,” www.onsemi.com/download/data-sheet/pdf/ncv5707-d.pdf
- [12] “HTCP Heat Transfer Compound Plus Technical Bulletin,” Electrolube, www.electrolube.com, 11 January 2022.
- [13] [AN-9090](#) “Impact of DBC Oxidation on (A)SPM Module Performance,” **onsemi**, Sept. 2019.
- [14] **onsemi** Data Sheet FAN73832, “Half-Bridge Gate Drive IC,” www.onsemi.com/download/data-sheet/pdf/fan73832-d.pdf
- [15] **onsemi** Data Sheet FAN7191, “Automotive Grade Driver IC, High and Low Side 600V, 4.5A,” www.onsemi.com/download/data-sheet/pdf/fan7191-f085-d.pdf
- [16] ni.com, CompactRIO Controller, www.ni.com/en-us/shop/hardware/products/compact-rio-controller.html

Excel is registered trademarks of Microsoft Corporation. All other brand names and product names appearing in this document are registered trademarks or trademarks of their respective holders.

onsemi, **ONSEMI**, and other names, marks, and brands are registered and/or common law trademarks of Semiconductor Components Industries, LLC dba “**onsemi**” or its affiliates and/or subsidiaries in the United States and/or other countries. **onsemi** owns the rights to a number of patents, trademarks, copyrights, trade secrets, and other intellectual property. A listing of **onsemi**’s product/patent coverage may be accessed at www.onsemi.com/site/pdf/Patent-Marking.pdf. **onsemi** reserves the right to make changes at any time to any products or information herein, without notice. The information herein is provided “as-is” and **onsemi** makes no warranty, representation or guarantee regarding the accuracy of the information, product features, availability, functionality, or suitability of its products for any particular purpose, nor does **onsemi** assume any liability arising out of the application or use of any product or circuit, and specifically disclaims any and all liability, including without limitation special, consequential or incidental damages. Buyer is responsible for its products and applications using **onsemi** products, including compliance with all laws, regulations and safety requirements or standards, regardless of any support or applications information provided by **onsemi**. “Typical” parameters which may be provided in **onsemi** data sheets and/or specifications can and do vary in different applications and actual performance may vary over time. All operating parameters, including “Typicals” must be validated for each customer application by customer’s technical experts. **onsemi** does not convey any license under any of its intellectual property rights nor the rights of others. **onsemi** products are not designed, intended, or authorized for use as a critical component in life support systems or any FDA Class 3 medical devices or medical devices with a same or similar classification in a foreign jurisdiction or any devices intended for implantation in the human body. Should Buyer purchase or use **onsemi** products for any such unintended or unauthorized application, Buyer shall indemnify and hold **onsemi** and its officers, employees, subsidiaries, affiliates, and distributors harmless against all claims, costs, damages, and expenses, and reasonable attorney fees arising out of, directly or indirectly, any claim of personal injury or death associated with such unintended or unauthorized use, even if such claim alleges that **onsemi** was negligent regarding the design or manufacture of the part. **onsemi** is an Equal Opportunity/Affirmative Action Employer. This literature is subject to all applicable copyright laws and is not for resale in any manner.

PUBLICATION ORDERING INFORMATION

LITERATURE FULFILLMENT:
Email Requests to: orderlit@onsemi.com

onsemi Website: www.onsemi.com

TECHNICAL SUPPORT
North American Technical Support:
Voice Mail: 1 800-282-9855 Toll Free USA/Canada
Phone: 011 421 33 790 2910

Europe, Middle East and Africa Technical Support:
Phone: 00421 33 790 2910
For additional information, please contact your local Sales Representative